Phytochemistry 206 (2023) 113560

Contents lists available at ScienceDirect

Phytochemistry

journal homepage: www.elsevier.com/locate/phytochem

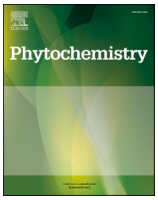

# Lipidomes of Icelandic bryophytes and screening of high contents of polyunsaturated fatty acids by using lipidomics approach

Yi Lu [a,b], Finnur Freyr Eiriksson [b,c], Margrét Thorsteinsdóttir [b,c], Nils Cronberg [d], Henrik Toft Simonsen [a,e,*]

[a] Department of Biotechnology and Biomedicine, Technical University of Denmark, Kongens Lyngby, Denmark
[b] ArcticMass, Reykjavik, Iceland
[c] Faculty of Pharmaceutical Sciences, University of Iceland, Reykjavik, Iceland
[d] Department of Biology, Lund University, Lund, Sweden
[e] Université Jean Monnet Saint-Etienne, CNRS, LBVpam UMR 5079, Saint-Étienne, France

ARTICLE INFO

*Keywords:*
Bryophytes
Mosses
Liverworts
Lipidomics
Polyunsaturated fatty acids
Mass spectrometry

ABSTRACT

Bryophytes (mosses, liverworts, and hornworts) have interested researchers because of their high chemical diversity and their potential uses in pharmaceutical, food, and cosmetic industries. Specifically, long-chain polyunsaturated fatty acids (l-PUFA) such as arachidonic acid (AA) and eicosapentaenoic acid (EPA) are commonly found in bryophytes, but not in vascular plants. Bryophytes accumulate PUFAs in cold or even freezing temperature to keep the cell fluidity. Iceland has a long history of bryophyte vegetation. These bryophytes are highly adapted to the harsh environment in Iceland and therefore are expected to produce high amounts of PUFAs. However, despite the fact that hundreds of mosses and liverworts have been found in Iceland, their lipid profiles largely remain unknown. In this study, we performed untargeted lipidomics by using UPLC-ESI-QTOF-MS as a rapid screening strategy to examine the lipid compositions of 39 local bryophyte species in Iceland and aimed to find high AA and EPA producers. A total of 280 lipid molecular species from 15 lipid classes were quantified with isotope-labeled internal standards. AA and EPA were abundantly distributed in the phospholipids (mainly PC and PE) and glycerolipids (MGDG and DGDG) in six moss species, namely *Racomotrium lanuginosum*, *R. ericoides*, *Bryum psedotriquetrium*, *Plagiomnium ellipticum*, *Hylocomium splendens*, and *Rhytidiadelphus triquetrus*. Two of the six species (*B. psedotriquetrium* and *H. splendens*) also accumulated high concentrations of PUFA-containing-triacylglycerols.

## 1. Introduction

Bryophytes are the second largest group of terrestrial plants and are divided into three subgroups – mosses, liverworts and hornworts (Horn et al., 2021). Bryophytes (especially mosses) have a long and successful colonization history in Iceland with *Racomitrium* being the most abundant genus (Ingimundardóttir et al., 2014). Notably, Icelandic bryophytes are well adapted to a very harsh environment as they grow in low temperatures almost all year around. The average temperature in Reykjavik is around 1 °C in winter and 12 °C in summer (Icelandic Meteorological Office, 2021). Under such circumstances, Icelandic bryophytes are expected to produce a considerable amount of PUFAs throughout the annual cycle. To date, 460 moss species, 139 liverwort species and one hornwort have been identified in Iceland (Icelandic Institute of Natural History, 2018). However, the lipid composition of Icelandic bryophytes is still poorly investigated.

Since a lot of studies of bryophytes have been focusing on volatile secondary metabolites, most of the chemical analysis has been performed with gas chromatography (GC) methods. GC-derived analytical methods are classical and robust as they can provide full-structural qualification and absolute quantification of a broad range of molecules including fatty acids (FAs). However, GC-based methods have several limitations. Only characterization and quantification of simple lipids such as free fatty acids and sterols can be obtained by GC-derived method (Christie and Han, 2012; Holčapek et al., 2018; Okazaki and Saito, 2018). Thus, recent studies have been focusing on lipid profiling using liquid chromatography-mass spectrometry (LC-MS) to provide an overview of the lipid species diversity in organisms including bryophytes.

* Corresponding author.
*E-mail addresses:* luyi.lucy@hotmail.com (Y. Lu), henrik.toft.simonsen@univ-st-etienne.fr (H.T. Simonsen).

https://doi.org/10.1016/j.phytochem.2022.113560
Received 15 September 2022; Received in revised form 8 December 2022; Accepted 10 December 2022
Available online 14 December 2022

**Abbreviations**

| | |
|---|---|
| l-PUFA | long-chain poly-unsaturated fatty acid |
| FA | fatty acid |
| AA | arachidonic acid |
| EPA | eicosapentaenoic acid |
| UPLC | ultra-performance liquid chromatography |
| UPLC-ESI-QTOF-MS | ultra-performance liquid chromatography-electrospray ionization-quadrupole time-of- flight mass spectrometry |
| GC | gas chromatography |
| TLC | thin layer chromatography |
| SPE | solid phase extraction |
| DDA | data dependent acquisition |
| DIA | data independent acquisition |
| PC | phosphatidylcholine |
| PE | phosphatidylethanolamine |
| PG | phosphatidylglycerol |
| PI | phosphatidylinositol |
| PA | phasphatidic acid |
| MGDG | monogalactosyldiacylglycerol |
| DGDG | digalactosyldiacylglycerol |
| SQDG | sulfoquinovosyldiacylglyceride |
| DGTS | diacylglycerol-o-(n,n,n-trimethyl)-homoserine |
| DG | diacylglycerol |
| TG | triacylglycerol |
| LPC | lyso-phosphatidylcholine |
| LPE | lyso-phosphatidylethanolamine |
| Cer | ceramide |
| SM | sphingomyelin |
| HexCer | hexosylceramide |
| QC | quality control |
| PCA | principal component analysis |
| PLS-DA | partial least-squares discriminant analysis |
| LC-MS | liquid chromatography-mass spectrometry |

The common fatty acids (FA) present in plants are 16:0, 18:1, 18:2, and 18:3. In addition to these common FAs, bryophytes produce considerable amounts of long-chain polyunsaturated fatty acids (l-PUFAs, ≤18 carbon chains) such as arachidonic acid (AA, 20:4, ω-6) and eicosapentaenoic acid (EPA, 20:5, ω-3) (Al-Hasan et al., 1989; Beike et al., 2014; Gellerman et al., 1975; Hartmann et al., 1986; Lu et al., 2019; Pejin et al., 2011). In general, bryophytes can survive in low temperature and harsh environment by accumulating FAs with longer and more unsaturated carbon chains in order to lower the solidification points. Hansen and Rossi (1990)examined the fatty acid composition of 25 moss species in the family Brachytheciaceae and Hypnaceae, the gametophytes of which contain up to 37% and 23% of total fatty acids of AA and EPA, respectively. Pejin et al. (2011)found that AA is the major fatty acid (30.7% of total FA) in *Rhytidiadelphus squarrosus* (Hedw.) Warnst. The AA and EPA content were observed to increase when the temperature dropped from 30 to 10° in cultured *R. squarrosus* and *Eurhynchium striatum* (Hansen and Rossi, 1991).

L-PUFAs (especially ω-3 PUFA) play an important role in human diet as they possess anti-inflammatory and antioxidant properties, and they are also highly associated with brain and retinal development in humans (Gupta et al., 2012). Since crops and other higher plants rarely contain l-PUFAs, the current source of l-PUFAs used as food supplements comes from marine fish oils or algae. However, fish and fish oils is not a sustainable source due to the decline of fish population and the accumulation of heavy metals in marine organisms (Jiao and Zhang, 2013). Algal oil is an alternative to both PUFA and l-PUFA, though the production cost is relatively high (Wijffels and Barbosa, 2010). Searching for an alternative source of l-PUFAs could help to lower the cost of EPA and AA (Lu et al., 2019). Bryophytes may not only provide a new edible source of PUFAs and l-PUFAs for human, they can also be targeted for promising transgenic approaches, e.g., for the optimization of oil seed crops to increase the amount of essential PUFAs and increase omega 3/6 ratio for human diet (Jiao and Zhang, 2013).

In this study, we examined the global lipidomes of 39 bryophyte species including 32 mosses and 7 liverworts from 10 orders, growing wild in Iceland using liquid chromatography-mass spectrometry (LC-MS)-based untargeted lipidomics approach. 2139 features were detected in positive electrospray ionization mode (ESI+) and 880 in negative electrospray ionization mode (ESI-). By using the *in silico* library LipidBlast, 603 and 322, in ESI+ and ESI- mode respectively, were identified as lipids. Multivariate statistical analysis and Hierarchical clustering analysis (HCA) were performed to discriminate the examined bryophyte species. Relative quantification of 15 lipid classes was achieved using isotope-labeled internal standards. Six moss species were found to contain high amounts of AA and EPA in the phosphor- and glycerolipids. Two of these six species also accumulated high concentration of triacylglycerol (TG) which contain AA and EPA.

### 1.1. Results and discussion

#### 1.1.1. Investigating the data quality

The MS/MS results were aligned and all possible peaks were detected. These data were then assigned to unique alignment IDs with their retention times and mass-to-charge ratios in both ESI+ and ESI- modes, respectively. In total, 2139 features were detected in ESI + mode and 880 in ESI- mode. All features with their raw peak areas were imported to SIMCA software. Here a PCA were performed to examine the species separation and to evaluate the quality of the dataset. The PCA plots were colored according to the sample type (sample or QC). A total of 25 QC samples are well clustered together in both modes (Fig. 1), even though the first two components of the PCA explain a comparatively low percentage of the variance for both modes (ESI+: PC1 = 8.27%, PC2 = 8.14%; ESI-: PC1 = 18.9%, PC2 = 8.56%). Overlapped chromatograms of all QC samples are displayed in Supplementary Fig. S1. Histograms of the distributions of coefficient of variances (CVs) of detected features are shown in Supplementary Fig. S2. 42% and 60% of the features in ESI+ and ESI- mode, respectively, from the QC samples have a less than 30% CV (Kaiser et al., 2011). Altogether, the datasets can be considered as of good quality and are reliable for further processing.

#### 1.1.2. PLS-DA

We further used PLS-DA models to determine the differences between all bryophyte species (Fig. 2). All detected features (i.e. all annotated lipids and other unidentified lipophilic and semi-lipophilic compounds) were included for discriminating the bryophyte species in ESI+ and ESI- mode, respectively. Both models were cross-validated with 100 permutation tests (Supplementary Fig. S3). In general, species belonging to the same order show similar lipid profiles.

In the first two components, all liverwort species (*Marchantia polymorpha*, *Chiloscyphus polyanthos*, *Tritomaria* sp., and *Scapania* sp.) are discriminated from all moss species. Moss species belonging to Grimmiales order (including *Racomitrium ericoides, R. lanuginosum, R. elongatum, and R. punctatum*) are separated from the rest of the moss species in ESI + mode, while *Pogonatum urnigerum* (order Polytrichales) is separated from the other mosses in ESI- mode. The loading plots displaying features contributing to the group separation in the score plots can be found in Supplementary Figs. S4 and S5. The features are colored by their retention times (RT) and mass-to charge-ratios (m/z),

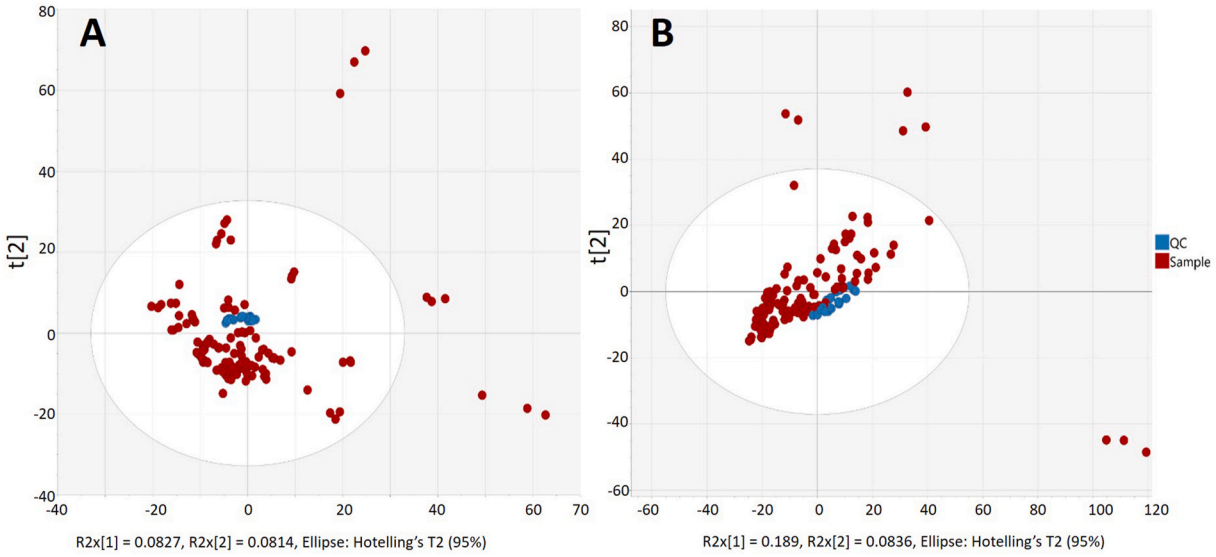


**Fig. 1.** Principle component analysis (PCA) of A). ESI+ (R2X = 0.802, Q2X = 0.344) and B). ESI- mode (R2X = 0.885, Q2X = 0.365) of overall dataset.

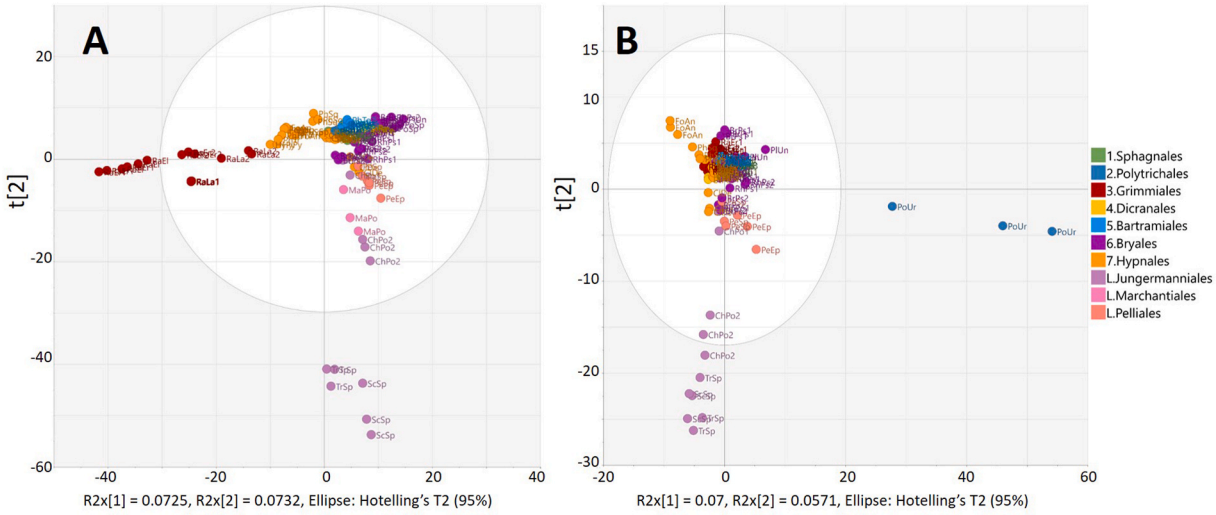


**Fig. 2.** PLS-DA score plots of 39 bryophyte species (n = 3) based on all detected features in A). ESI+ (R2X = 0.694, R2Y = 0.931, Q2 = 0.699) and B). ESI-mode (R2X = 0.625, R2Y = 0.907, Q2 = 0.647), respectively. The bryophytes species are displayed as dots and colored according to the phylogenetic order they belong to as indicated in the legend. The order that begins with a number (1–7) indicates the phylogenetic order of mosses whereas the order that begins with "L" indicates liverworts. The codes of the species can be seen in Table 1.

respectively, in the loading plots. The outlier groups were compared to the average observations, and the top 10 features with highest contribution scores are listed in Supplementary Figure S4C, D and S5C, D. The features that caused separations of different groups are mostly unidentified, which indicate that other lipophilic compounds than lipids could potentially be the biomarkers for the correspondent species. For example, liverworts are known to produce some unique compounds that mosses do not, like diverse terpenoids, bibenzyls, and bisbibenzyls (Asakawa et al., 2013; Asakawa and Ludwiczuk, 2018; Tosun et al., 2015). High contents of TG 18:3_18:3_18:3 might be a chemical marker for the *Racomitrium* species (Supplementary Fig. S4C), which was also observed previously (Lu et al., 2021). However, the variations of 14.57% in ESI+, and 12.71% in ESI- mode, are explained in the first two components in the PLS-DA models. This suggests the lipid profiles are relative similar within bryophytes, and the differences are relatively small.

### 1.1.3. *Chemotaxonomic relationships between examined species*

In order to perform chemotaxonomic analysis of the examined species based on their chemical profiles, features detected in ESI + mode and ESI- mode were combined into a single data matrix and imported to SIMCA. HCA was constructed based on a new PLS-DA model using the combined data matrix (Fig. 3).

Sphagnales and Hypnales show a close relationship based on their MS/MS profiles, with the exception of *Fontinalis antipyretica*, which has a closer relationship with Grimmiales. This could be explained by the significant higher concentration of TG in *F. antipyretica* compared to the rest of the species in Hypnales order (Fig. 4). For instance, the most abundant TG lipid 54:7 is up to 15,000 μmol/mg dry weight in *F. antipyretica*, while the concentration of the same lipid in the rest of the species in Hypnales (e.g., *Hylocomiastrum pyrenaicum*) is almost 10 times less (Supplementary Fig. S6). All species in Bryale and Bartramiales order are clustered together, indicating their similar lipid profiles.

In order to compare the chemotaxonomic similarity of examined bryophyte species to their phylogenetic relationships, the species included in this study were extracted from Open Tree of Life (node ID: mrcaott541ott1066, Redelings and Holder, 2017). The phylogenetic tree

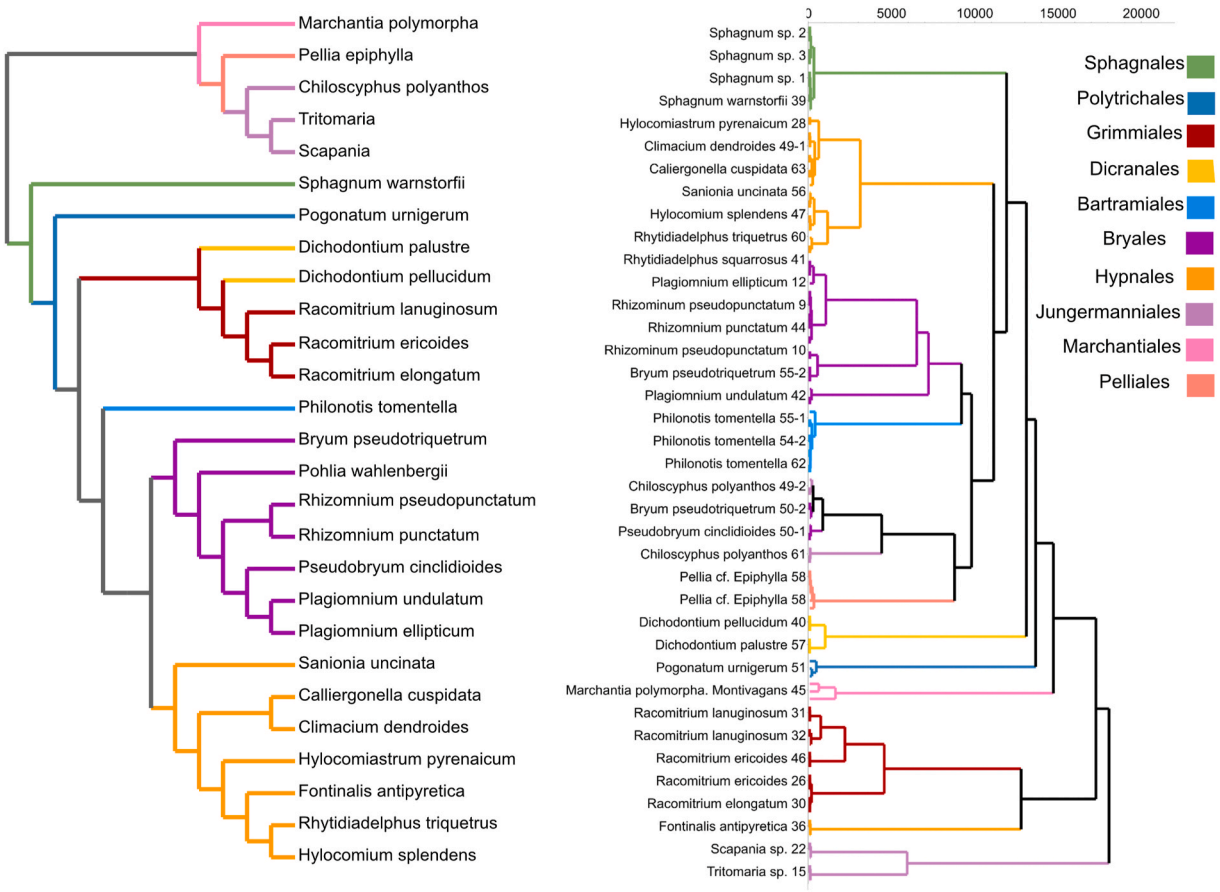


**Fig. 3.** (A). Phylogenetic tree reconstructed from Open Tree of Life compared to (B). Chemotaxonomic relationships of combined ESI+ and ESI- modes features of included bryophyte species. The branches are colored according to the species phylogeny orders. Hierarchical distance of (B) is calculated with Ward method and sorted by index (n = 3).

from Open Tree of Life contains distance relationships from multiple existing genomic and metabolic sources (Laurin-Lemay et al., 2012; Parfrey et al., 2011; Ruhfel et al., 2014). Species in Bartramiales, Bryales and Hypnales order show close relationships in both phylogenetic and chemotaxonomic relationships, whereas the liverworts are not distinguished as a separate lineage in the chemotaxonomic discrimination, except for *Scapania* sp. And *Tritomatia* sp. Overall the chemical clustering follow the genetic clustering, with small differences, but further studies would be needed to clarify these.

Previous studies have used chemotaxonomic analysis to discriminate plant phenotypes using LC-MS-based and/or GC-MS-based metabolite profiling (Arbona et al., 2009; Liu et al., 2020), and fatty acid profiles (Choudhary et al., 2017). Recently, this method have also been applied to bryophytes to explore the chemotaxonomic differentiations by their fatty acid profiles (Poddar Sarkar et al., 2021) and by chemical profiles (Peters et al., 2021). Compared to the traditional DNA sequencing method, chemotaxonomic analyses based on MS/MS spectra is relatively inexpensive (Peters et al., 2021). However, in order to get a full picture of the chemodiversity of the bryophytes, hydrophobic compounds should also be included, and the species should be collected different locations and time, in order to compensate for the environmental factors (or grown in vitro).

### *1.1.4. Lipid profiles of 39 bryophyte species with a focus on AA and EPA*

To annotate lipid features the *in silico* library LipidBlast was used. A total of 602 out of 2139 features was annotated in ESI+ mode, and 322 out of 880 features in ESI- mode, respectively (Supplementary Data 2). A total of 15 lipid classes were characterized in the whole dataset, and show the fatty acid distribution of six species (*R. lanuginosum* 39, *R. ericoides* 46, *B. pseudotriquetrum* 55–2, *P. ellipticum* 12, *H. splendens* 47, *R. triquetrus* 60) that show high levels of AA (20:4) and EPA (20:5) (Fig. 5). Since lipids from different lipid classes have different ion efficiency, and IS for glycerolipids quantification is lacking, the appearances of fatty acids in each lipid class was counted instead of using the ion intensities (Tsugawa et al., 2019b). Barplots of fatty acid distributions of all lipid classes (except for TG) in each bryophyte species can be found in Supplementary Fig. S7. Since TG lipids have more combinations of the fatty acyl moieties than other lipids, and the MS/MS spectrums in DIA mode are usually "mixed" with multiple compounds, false-positive identifications may occur when identifying the TG lipids in fatty acyl level. Thus, an annotation was performed on the molecular species with total carbon numbers and total unsaturation degrees within TG lipid class (Tsugawa et al., 2019b). The TG concentrations of selected six species is shown in Fig. 6. Barplots of TG concentrations in all bryophyte species can be found in Supplementary Fig. S6. In order to find species that produce relative high levels of l-PUFA, the lipid molecular species was quantified from each 15 lipid classes by using the mixture of the IS added prior to the lipid extraction. Relative quantification of all identified lipid molecular species is displayed in Fig. 4. The major fatty acids present in all species and samples are 16:0, 18:1, 18:2, 18:3, 20:4, and 20:5, and also minor 16:1, 16:2, and 16:3. This is in agreement with most of the previous studies (Beike et al., 2014; Dembitsky and Rezanka, 1995; Hansen Patricia Rossi, 1990). 16:0 is the most common fatty acid in all examined bryophyte species except for samples of *R. ericoides* 46, *Hylocomium splendens* 47, and *Rhytidiadelphus triquetrus* 60, in which the counts of 18:3 surpass 16:0 (Fig. 5). High abundance of 18:3 in *R. ericoides* 46 is also accumulated in TG as storage lipids. Like indicated in the PLS-DA models previously, the *Racomitrium*

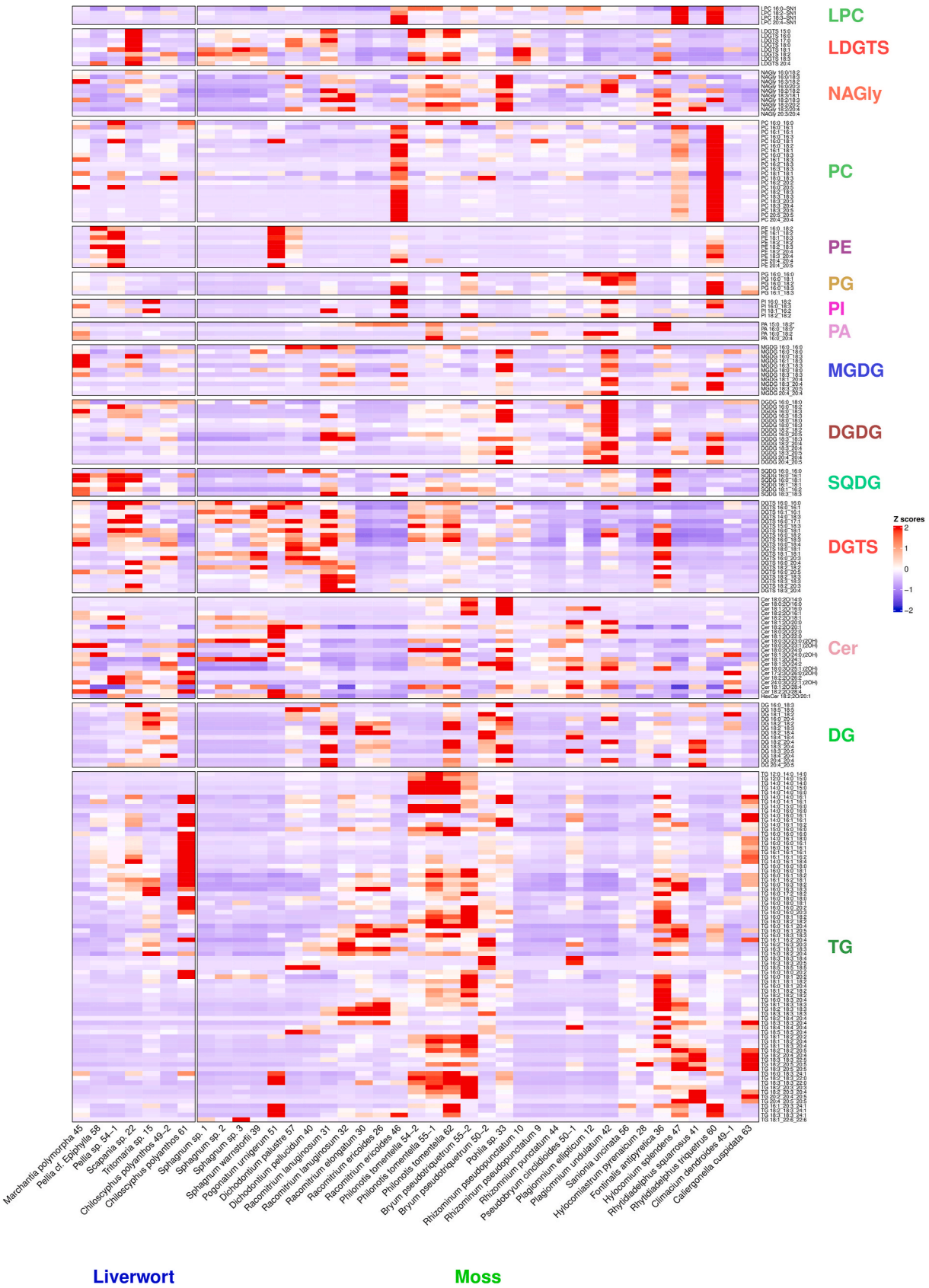


**Fig. 4.** Heatmap of relative concentrations of all identified lipid molecular species from 39 bryophyte species. The lipid molecular species are grouped and colored by the lipid classes. The order of the bryophyte species is manually set to follow the phylogenetic order. The concentrations are log-transformed and Z-score is used to display the abundance of the lipids.

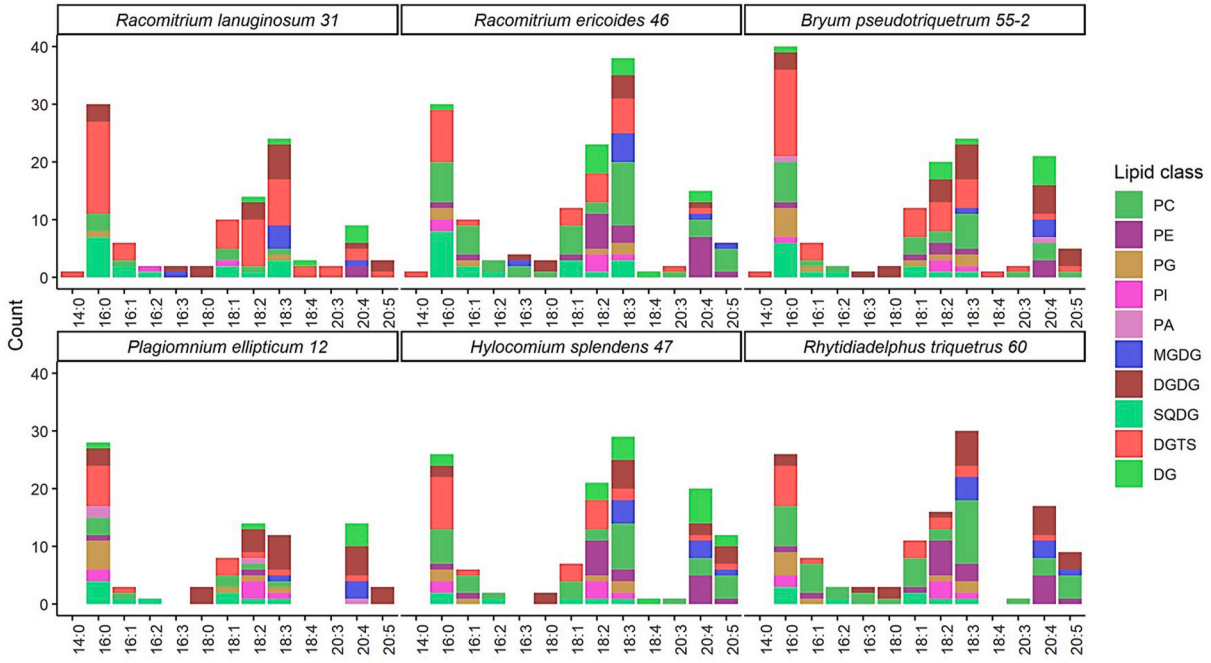


**Fig. 5.** Fatty acid distributions of *R. lanuginosum* 39, *R. ericoides* 46, *B. pseudotriquetrum* 55–2, *P. ellipticum* 12, *H. splendens* 47, *R. triquetrus* 60, all with high levels of 20:4 and 20:5 in 10 lipid classes including phospholipid (PC, PE, PG, PI, and PA), glycerolipids (MGDG, DGDG, SQDG, and DGTS)), and DG. A full fatty acid distribution of all examined species can be found in Supplementary Fig. S7.

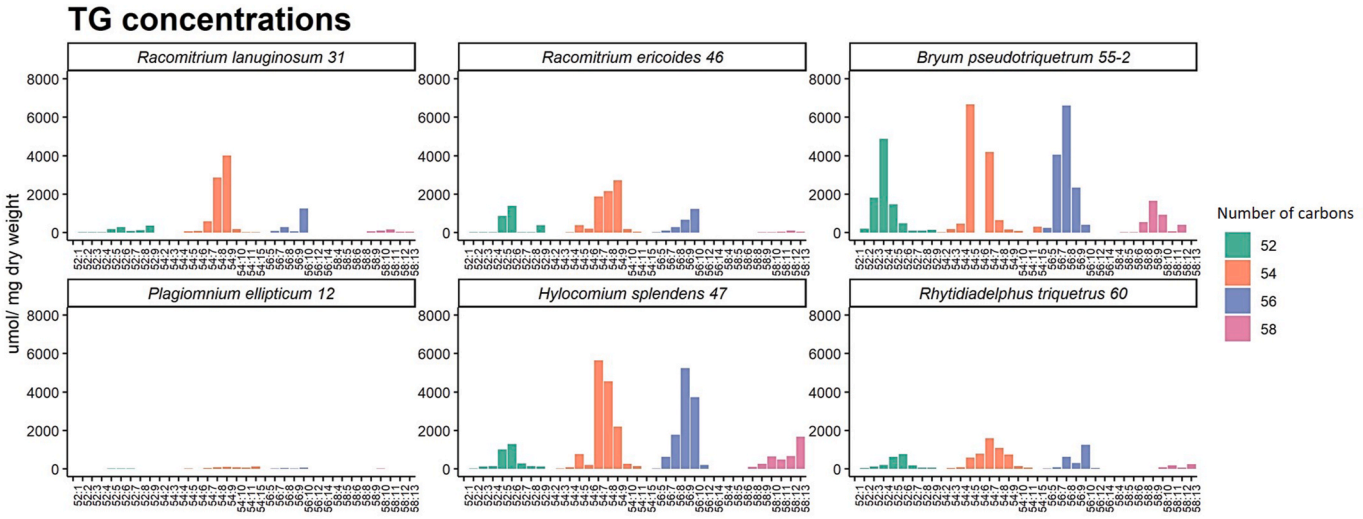


**Fig. 6.** Investigation of the TG concentrations of *R. lanuginosum* 39, *R. ericoides* 46, *B. pseudotriquetrum* 55–2, *P. ellipticum* 12, *H. splendens* 47, *R. triquetrus* 60, all with high levels of 20:4 and 20:5 fatty acids. The concentration is calculated by using the internal standard TG and normalized by the dry weight (mg) in individual samples (n = 3). A full TG concentration of all examined species can be found in Supplementary Fig. S6. Carbon numbers less than 52 and larger than 58 are excluded as they are present in low abundance in all species.

species are enriched in TG 54:9 (TG 18:3_18:3_18:3). Together with other l-PUFAs (20:4 and 20:5) present in the phospho- and glycerolipids, these constituents enable *Racomitrium* species to survive in cold environment, and could explain the high coverage of *Racomitrium* species in Iceland vegetation (Icelandic Institute of Natural History, 2018). Interestingly, although in minor amount, 18:0 is found in most of the species in the form of DGDG 18:0_18:3. Previous studies show that saturated fatty acyls such as 18:0 are usually not observed in glycerolipids in plants or algae (Kilaru et al., 2012; Tsugawa et al., 2019b). Here, both the common 16:0 and more uncommon 18:0 are found in MGDG and DGDG as one of the fatty acyls, together with another unsaturated fatty acyls (e.g., MGDG 16:0_18:3, DGDG 16:0_18:3, and DGDG 18:0_18:3) (Fig. 4).

In *R. ericoides* 46, *Bryum psedotriquetrium* 55–2, *H. splendens* 47, and *R. triquetrus* 60, the l-PUFAs (20:4 and 20:5) are mainly distributed in PE and PC lipid classes (Fig. 5), but only *R. ericoides* 46 and *R. triquetrus* 60 contain high relative concentrations of PE and PC lipids with 20:4 and 20:5 (Fig. 4). Meanwhile, although *Plagiomnium ellipticum* 12 shows high abundance of 20:4 and 20:5 in the phosphor- and glycerolipids, it produces much lower TG as storage lipids compared to the other five moss species (Fig. 6).

High abundances of 20:4 and 20:5 fatty acids can be observed in *B. psedotriquetrum* 55–2 in most of the lipid classes (Fig. 5). The TG profile of this species also shows high amounts of TG with more than 56

carbon numbers and more than 8 unsaturation degrees, which indicates that at least one l-PUFA is present in these TG molecular species (e.g., TG 56:8 can represent TG 18:1_18:3_20:4) (Fig. 6). These results suggest that *B. psedotriquetrum* could be an optimal species for producing l-PUFAs. It is also worth to notice that another sample, *B. psedotriquetrum* 50–2, contains almost no l-PUFAs in the phosphor- and glycerolipids (Supplementary Fig. S7). Moreover, *B. psedotriquetrum* 50–2 produces lower concentrations of TG that are likely to contain l-PUFAs (Supplementary Fig. S6), showing that the environmental factors need to be examined further if the species is to be used for production.

Similar examples of infraspecific variation can also be seen in the liverworts. For example, *C. polyanthos* 49–2 produces more lipid species and higher concentrations of TG lipids with 54 carbons than *C. polyanthos* 61, whereas *C. polyanthos* 61 is richer in TG lipids with 52 carbons. The same species collected at different site were likely exposed to contrasting stress or microclimatic conditions, and therefore, display different lipid profiles.

The betaine lipid DGTS is widely distributed in all examined bryophytes with most of the common fatty acyl chains (16:0, 18:1, 18:2, and 18:3) (Fig. 4, Supplementary Fig. S7). Unlike vascular plants, in which PC is the most common membrane component, DGTS has earlier been found in algae species (e.g., *Chlorococcum amblystomatis*, *Sargassum horneri*, and diatom *Conticribra weissflogi*) (Conde et al., 2021; Li et al., 2016; Zhang et al., 2018), as well as in other early divergent plants including bryophytes and ferns (Künzler and Eichenberger, 1997; Mikami and Hartmann, 2004). DGTS is also reported in other organisms such as lichen and fungi (Celis Ramírez et al., 2020; Künzler and Eichenberger, 1997; Yang et al., 2021). Studies show a reciprocal relationship between PC and DGTS, which imply that DGTS serves as a replacement for PC in the lipid membranes when nutrients are limited (Yang et al., 2015). This is supported by results shown here where species enriched in PC, generally have low abundance of DGTS, and vice versa (e.g., *R. ericoides* 46, *H. splendens* 47, and *R. triquetrus* 60) (Fig. 4). As a primary lipid, DGTS is gradually replaced by PC during the evolution, and DGTS is absent in vascular plants (Cannell et al., 2020). Among representatives of the deeply rooted moss lineages Sphagnales (*Sphagnum* spp.) and Polytrichales (*Pogonatum*), as well as the genus *Dichodontium*, DGTS represents the major lipid class, whereas PC is almost absent, which implies that acquisition of PC in the membrane lipid synthesis pathway may represent a derived trait. The widely distributed DGTS in all species may also reflect the low phosphorus levels in Iceland (OECD, 2013), The fatty acid 18:5 is only present in the form of DG (18:5_18:5) and TG (18:5_18:5_18:5 and 18:5_18:5_20:4) in *Dichodotium palustre* 57 and *D. pellucidum* 40, but not present in any forms of the phosphor- and glycerolipids (Fig. 4). Remarkable high amounts of TG 54:15 (TG 18:5_18:5_18:5) are accumulated in *D. palustre* 57 (25,000 μmol/mg dry weight) and *D. pellucidum* 40 (12,000 μmol/mg dry weight). Such high concentration of 18:5 is uncommon in any other examined species. In this study, lipid identification is only conducted in fatty acyl levels, therefore, the stereochemistry of the fatty acyl chain is unknown. However, the detected 18:5 could be the acetylenic fatty acid dicranin (octadeca-6-yn-9,12,15-trienoic acid), instead of polyunsaturated fatty acid octadecapentaenoic acid, as dicranin is confirmed to be a biochemical marker of Dicranaceae, produced in response to environmental stress (Dembitsky and Rezanka, 1994; Lu et al., 2019; Poddar Sarkar et al., 2021; Roy Chowdhuri et al., 2018).

Compared to the traditional Data Dependent Acquisition (DDA) method, untargeted lipidomics analysis using DIA will provide as many features as possible based on the MS/MS spectra. Low abundance compound can also be quantified with high precision, even though the compound annotation might be challenging (Tsugawa et al., 2019b). In this study, only 28% and 36% of the detected features were successfully identified in ESI+ and ESI- mode, respectively. The rest of the lipophilic and semi-lipophilic features remain unannotated here. Future studies could potentially identify the remaining unknown features by searching the obtained spectra in other databases such as MassBank, Metlin, and GNPS (Horai et al., 2010; Smith et al., 2005; Wang et al., 2016), and/or by using advanced *in silico* data analysis methodologies such as MetFamily, SIRIUS, and MS-FINDER (Dührkop et al., 2019; Peters et al., 2019; Tsugawa et al., 2019a).

## 2. Conclusion

In this study, we conducted untargeted lipidomic analysis by using UPLC-ESI-QTOF-MS with data independent acquisition of 39 bryophyte species including 32 mosses and 7 liverworts. Six moss species *Racomotrium lanuginosum*, *R. ericoides*, *B. psedotriquetrium*, *P. ellipticum*, *H. splendens*, and *R. triquetrus* showed high abundance of arachidonic acid (20:4) and eicosapentaenoic acid (20:5) in the form of phospholipids and glycerolipids. In the TG profiles of these species, *P. ellipticum* had the lowest concentrations of TG lipids with 52–58 total carbon numbers, while *B. psedotriquetrium* and *H. splendens* accumulate up to 6000 μmol/mg dry weight of TG with high unsaturation degrees. Thus, *B. psedotriquetrium* and *H. splendens* could be potential future PUFA sources, though the impact of the environmental factors (e.g., temperature, habitat, and pH, etc.) was not included in this study. It is known that the environmental factors can promote or inhibit the PUFA production. Future investigations of the changes of lipid profiles under various environmental conditions, and in vitro performance of those species are needed. This study provides a better understanding of the lipid fingerprints of a wide range of bryophyte species for future bryologists.

## 3. Experimental

### 3.1. Chemicals

Potassium chloride (KCl, purity ≥99.0%), HPLC grade chloroform and methanol (for lipid extraction); LC–MS grade acetonitrile, isopropanol and ammonium acetate, were purchased from Sigma; Milli-Q water was used for lipid extraction and for UPLC-ESI-QTOF-MS analysis. Glass tube with PTFE coated screw caps was used for lipid extraction.

### 3.2. Sample collection and species identification

We collected 39 bryophyte species (32 mosses and 7 liverworts) in Iceland in summer between June to August 2018 and 2019. A detailed list with collection sites and their exact coordinates is shown in Table 1. The average temperature during collection was around 8–10 °C in 2018 and around 19 °C in 2019. Samples were stored in Ziploc plastic bags and kept on ice to maintain the freshness. After collection, the samples were transported to the laboratory as soon as possible and washed thoroughly with de-ionized water. The cleaned material was stored at −80 °C until further processing.

Species were identified by Nils Cronberg, Lund University. Voucher specimens were prepared by drying a small amount of the collected species at ambient room temperature without direct sun exposure. The voucher specimens were deposited at Lund University.

### 3.3. Lipid extraction

Lipids were extracted by using the Folch method with a few modifications as described in our previous publication (Folch et al., 1957; Lu et al., 2021). Briefly, fresh plant material was first crushed in liquid nitrogen, ~100 mg pulverized powder (in case of mosses, only the aboveground green parts were used for extraction) was weighed into a glass tube. 3 mL chloroform/methanol (2:1, v/v) containing a mixture of internal standard (IS) was added into the tube, the mixture was vortexed thoroughly and kept on ultrasound for 20 min at room temperature. Subsequently, 0.75 mL 1 M KCl was added to the glass tube, agitated, and centrifuged at 1000 g for 5 min at 4 °C. The chloroform phase was

**Table 1**
Collected and examined bryophyte samples, with names, voucher number (including sample number used in other figures), date and the locations of collection.

| Species | Family | Voucher ID. | Collection site | Date | N-coordinate | E-coordinate | Code |
|---|---|---|---|---|---|---|---|
| *Bryum pseudotriquetrum* (Hedw.) P.Gaertn., B. Mey. & Scherb. | Bryaceae | MTYiLu50-2 | Kaldbaksvegur, Hruni | 12/06-2019 | 64.1585 | −20.1920 | BrPs2 |
| *Bryum pseudotriquetrum* (Hedw.) P.Gaertn., B. Mey. & Scherb. | Bryaceae | MTYiLu55-2 | Road F338, Hruni | 13/06-2019 | 64.3729 | −20.1376 | BrPs1 |
| *Calliergonella cuspidate* (Hedw.) Loeske | Amblystegiaceae | MTYiLu63 | Vatnaleið, Eyja- og Miklaholtshreppur | 14/06-2019 | 64.2609 | −21.3707 | CaCu |
| *Chiloscyphus polyanthos* (L.) Corda | Lophocolea-ceae | MTYiLu49-2 | Kaldbaksvegur, Hruni | 12/06-2019 | 64.1586 | −20.1918 | ChPo1 |
| *Chiloscyphus polyanthos* (L.) Corda | Lophocolea-ceae | MTYiLu61 | þórufoss | 13/06-2019 | 64.3274 | −20.2859 | ChPo2 |
| *Climacium dendroides* (Hedw.) F.Weber & D.Mohr | Climaciaceae | MTYiLu49-1 | Kaldbaksvegur, Hruni | 12/06-2019 | 64.1586 | −20.1918 | ClDe |
| *Dichodontium palustre* (Dicks.) M.Stech | Dicranaceae | MTYiLu57 | Road F338, Hruni | 13/06-2019 | 64.3729 | −20.1376 | DiPa |
| *Dichodontium pellucidum* (Hedw.) Schimp. | Dicranaceae | MTYiLu40 | Tumastaðir | 02/09-2018 | 64.7173 | −14.4008 | DiPe |
| *Fontinalis antipyretica* Hedw. | Fontinala-ceae | MTYiLu36 | þjóðvegur, Djúpivogur | 02/09-2018 | 64.7173 | −14.4008 | FoAn |
| *Hylocomium pyrenaicum* (Spruce) Lindb. | Hylocomia-ceae | MTYiLu28 | Vatnaleið, Eyja- og Miklaholtshreppur | 29/08-2018 | 64.5916 | −21.9942 | HyPy |
| *Hylocomium splendens* (Hedw.) Schimp. | Hylocomia-ceae | MTYiLu47 | Kaldbaksvegur, Hruni | 12/06-2019 | 64.1420 | −20.2344 | HySp |
| *Marchantia alpestris*(Nees) Burgeff | Marchantia-ceae | MTYiLu45 | Kaldbaksvegur, Hruni | 01/09-2018 | 65.6389 | −16.8071 | MaPo |
| *Pellia epiphylla* (L.) Corda | Pelliacaea | MTYiLu58 | Haukadalsskógur | 13/06-2019 | 64.3729 | −20.1376 | PeEp |
| *Pellia* L. *sp.* | Pelliacaea | MTYiLu54-1 | Road F338, Hruni | 13/06-2019 | 64.3729 | −20.1376 | PeSp |
| *Philonotis tomentella* Molendo | Bartramia-ceae | MTYiLu62-1 | þórufoss | 14/06-2019 | 64.2609 | −21.3707 | PhTo3 |
| *Philonotis tomentella* Molendo | Bartramia-ceae | MTYiLu54-2 | Road F338, Hruni | 13/06-2019 | 64.3729 | −20.1376 | PhTo1 |
| *Philonotis tomentella* Molendo | Bartramia-ceae | MTYiLu55-1 | Road F338, Hruni | 13/06-2019 | 64.3729 | −20.1376 | PhTo2 |
| *Plagiomnium ellipticum* (Brid.) T.J.Kop. | Mniaceae | MTYiLu12 | Vatnaleið, Eyja- og Miklaholtshreppur | 21/07-2018 | 64.9055 | −22.8568 | PlEl |
| *Plagiomnium undulatum* (Hedw.) T.J.Kop. | Mniaceae | MTYiLu42 | Tumastaðir | 03/09-2018 | 63.7401 | −20.0633 | PlUn |
| *Pogonatum urnigerum* (Hedw.) P.Beauv. | Polytricha-ceae | MYYiLu51 | Kaldbaksvegur, Hruni | 12/06-2019 | 64.1582 | −20.1923 | PoUr |
| *Pohlia* Hedw. *Sp.* | Mniaceae | MTYiLu33 | þjóðvegur, Djúpivogur | 01/09-2018 | 65.6389 | −16.8071 | PoSp |
| *Pseudobryum cinclidioides* (Huebener) T.J.Kop. | Mniaceae | MTYiLu50-1 | Kaldbaksvegur, Hruni | 12/06-2019 | 64.1585 | −20.1920 | PsCi |
| *Racomitrium elongatum*Ehrh. Ex Frisvoll | Grimmiaceae | MTYiLu30 | Hverir, Mývatn | 31/08-2018 | 65.5003 | −20.6801 | RaEl |
| *Racomitrium ericoides* Brid. | Grimmiaceae | MTYiLu26 | Borgarbyggd | 29/08-2018 | 64.5916 | −21.9942 | RaEr1 |
| *Racomitrium ericoides* Brid. | Grimmiaceae | MTYiLu46 | Kaldbaksvegur, Hruni | 12/06-2019 | 64.1420 | −20.2344 | RaEr2 |
| *Racomitrium lanuginosum* (Hedw.) Brid. | Grimmiaceae | MTYiLu31 | Hverir, Mývatn | 01/09-2018 | 65.6389 | −16.8071 | RaLa1 |
| *Rhizomnium pseudopunctatum* (Bruch & Schimp.) T.J.Kop. | Mniaceae | MTYiLu9 | Vatnaleið, Eyja- og Miklaholtshreppur | 21/07-2018 | 64.5912 | −21.9932 | RhPs1 |
| *Rhizomnium pseudopunctatum* (Bruch & Schimp.) T.J.Kop. | Mniaceae | MTYiLu10 | Vatnaleið, Eyja- og Miklaholtshreppur | 21/07-2018 | 64.9058 | −22.8573 | RhPs2 |
| *Rhizomnium punctatum* (Hedw.) T.J.Kop. | Mniaceae | MTYiLu44 | Hverir, Mývatn | 31/08-2018 | 65.5003 | −20.6801 | PhPu |
| *Rhytidiadelphus squarrosus* (Hedw.) Warnst. | Hylocomia-ceae | MTYiLu41 | Tumastaðir | 03/09-2018 | 63.7401 | −20.0633 | PhSq |
| *Rhytidiadelphus triquetrus* (Hedw.) Warnst. | Hylocomia-ceae | MTYiLu60 | Haukadalsskógur | 13/06-2019 | 64.3274 | −20.2859 | PhTr |
| *Sanionia uncinate* (Hedw.) Loeske | Amblystegiaceae | MTYiLu56 | Road F338, Hruni | 13/06-2019 | 64.3729 | −20.1376 | SaUn |
| *Scapania* (Dumort.) Dumort. *Sp.* | Scapaniaceae | MYYiLu22 | Borgarbyggd | 22/07-2018 | 64.5911 | −21.9930 | ScSp |
| *Sphagnum* L. *sp* | Sphagnaceae | MTYiLu2 | Vatnaleið, Eyja- og Miklaholtshreppur | 21/07-2018 | 64.9055 | −22.8568 | SpSp2 |
| *Sphagnum* L. *sp* | Sphagnaceae | MTYiLu3 | Borgarbyggd | 21/07-2018 | 64.9055 | −22.8568 | SpSp3 |
| *Sphagnum* L. *sp* | Sphagnaceae | MTYiLu1 | Vatnaleið, Eyja- og Miklaholtshreppur | 21/07-2018 | 64.9055 | −22.8568 | SpSp1 |
| *Sphagnum warnstorfii* Russow | Sphagnaceae | MTYiLu39 | þjóðvegur, Djúpivogur | | 64.7173 | −14.4008 | SpWa |

(*continued on next page*)

**Table 1** (*continued*)

| Species | Family | Voucher ID. | Collection site | Date | N-coordinate | E-coordinate | Code |
|---|---|---|---|---|---|---|---|
| *Tritomaria* Schiffn. Ex Loeske sp. | Lophozia-ceae | MTYiLu15 | Kjösarskarðsvegur | 02/09-2018 22/07-2018 | 64.2370 | −21.3513 | TrSp |

transferred carefully to a new glass tube by a Pasteur pipette. The remaining bryophyte material was washed twice with 1 mL chloroform, and the chloroform phase was collected to the new glass tube after centrifugation. The chloroform was evaporated under nitrogen gas and stored at −80 °C until analysis.

Since the bryophyte samples were collected in a wide range of different geographical locations, the water content of the samples may vary. In this case, we estimated the water content of each sample and normalized the variation by using dry weight (mg) (Antonio, 2018). Water content was calculated by dividing the water loss from the fresh material to the total weight of the sample. In brief, fresh material was weighed in a pre-weighed Eppendorf tube and dried in an oven at 60 °C until constant weight. The Eppendorf tube with dried bryophyte sample was weighed again to obtain the weight of the water loss.

### 3.4. UPLC-ESI-QTOF-MS analysis

The dried lipid residue was re-dissolved in 150 μL solvent mixture containing 1 part of chloroform/methanol (1:1, v/v) and 9 parts of isopropanol/acetonitrile/water (2:1:1, v/v/v), and filtered through a 0.22 μm pore size PTFE filter (Minispike Syringe Filter, Waters Corp., Milford, USA). The solution was injected to an ACQUITY UPLC (Waters Corp., Milford, USA) coupled with a quadruple time-of-flight hybrid mass spectrometry Synapt G1 (Waters Corp., Milford, USA) equipped with electrospray ionization (ESI) interface (Waters Corp., Milford, USA). Compound separation was performed on an ACQUITY UPLC HSS T3 reverse-phase column (2.1 mm × 100 mm × 1.8 μm, Waters). Mobile phase A consists of acetonitrile/water (60:40, v/v) and mobile phase B isopropanol/acetonitrile (90:10, v/v), both supplied with 10 mM ammonium acetate. The following linear gradient elution was applied: 0–10 min, 40–100% B; 10–12 min, 100% B; 12–14.5 min, reconditioning to 40% B. Flow rate was 0.4 mL/min and column temperature was 55 °C. Sample manager temperature was maintained at 10.0 °C.

Mass spectrometry (MS) was operated in V mode. MS Data was collected in both positive and negative ionization mode (ESI+ and ESI-). Injection volume was 2 μL in ESI + mode and 5 μL in ESI- mode. Mass was scanned in a range of 100–1500 Da. Data independent MS/MS acquisition (DIA) mode was applied. Collision energy was 10 eV for the MS1 acquisition and the MS2 acquisition had a collision energy ramp of 20–45 eV. Leucine encephalin (1 ng/μL) was used as reference lock mass calibrant ([M + H]+ ion of 556.2771 and [M-H]− ion of 554.2615). Other MS conditions are described in our previous study (Lu et al., 2021).

To detect the deviations of retention time shifts between batches and to ensure the performance of the instrument, the injection order was randomized. In addition, quality control (QC) was prepared by pooling 10 μL aliquots of all samples and the QC was injected to the system between every 12 samples, as well as at the start and the end of the analytical batch.

### 3.5. Data analysis

#### 3.5.1. Lipidomics data processing

Raw data from UPLC-ESI_QTOF-MS were converted to. abf format by using ABF Converter (Tsugawa et al., 2013) (https://www.reifycs.com/AbfConverter/), then imported to MS-DIAL, version 4.24 (http://prime.psc.riken.jp/compms/msdial/main.html) for performing peak detection, deconvolution, compound identification and alignment. The import parameters are listed in Supplementary data S1.

#### 3.5.2. Lipid identification

*In silico* library LipidBlast was used for identification as a part of the data processing procedure in MS-DIAL (Kind et al., 2013). The following lipid classes were investigated in this study: phosphatidylcholine (PC), phosphatidylethanolamine (PE), phosphatidylglycerol (PG), phosphatidylinositol (PI), phosphatidylserine (PS), phasphatidic acid (PA), monogalactosyldiacylglycerol (MGDG), digalactosyl diacylglycerol (DGDG), sulfoquinovosyldiacylglyceride (SQDG), diacylglyceryltrimethylhomoserine (DGTS), lysophosphatidylcholine (LPC), lysophosphatidylethanolamine (LPE), lysodiacylglyceryltrimethylhomoserine (LDGTS), diacylglycerol (DG), triacylglycerol (TG), N-acyl glycine (NAGly), ceramide (Cer), fatty acid (FA). Since DIA method provides all fragment ions from all precursors in MS/MS spectra, it might be difficult to obtain "clean" spectra purified from other co-eluting compounds. In order to reduce the false identification, all annotations were double-checked on the 2D map in MS-DIAL interface to visualize a systematic retention time shift when the carbon numbers and unsaturation levels change within the same lipid class (Antonio, 2018).

#### 3.5.3. Data normalization and relative quantification

The normalization was achieved by using a mixture of 12 isotope-labeled IS standards containing 20 μg/mL PC 15:0–18:1 (d7), 16 μg/mL PE 15:0–18:1 (d7), 10 μg/mL PG 15:0–18:1 (d7), 10 μg/mL PA 15:0–18:1 (d7), 10 μg/mL PI 15:0–18:1 (d7), 10 μg/mL PS 15:0–18:1 (d7),4 μg/mL LPC 18:1 (d7), 10 μg/mL LPE 18:1 (d7), 10 μg/mL DG 15:0–18:1 (d7), 4 μg/mL TG 15:0–18:1 (d7)-15:0, 5 μg/mL SM 18:1; 2O/18:1 (d9), and 5 μg/mL Cer 18:1; 2O/16:0 (d7). In general, the lipid quantification follows the "one standard per class" rule. However, since there are no available internal standards available commercially for the glycerolipids MGDG, DGDG, SQDG, and DGTS, SM 18:1; 2O/18:1 (d9) was used to calculate the quantifies of these lipid classes. Data sheet of raw areas of all detected features, together with normalized concentrations of all identified lipids are deposited in Supplementary Data S2.

#### 3.5.4. Further analysis and visualization

Principal component analysis (PCA) and partial least squares discriminant analysis (PLS-DA) were conducted in SIMCA 17 (Sartorius Stedim Data Analytics, Umeå, Sweden) using aligned results of raw area with unit variance (UV) scale (Bruce et al., 2008; Eriksson et al., 2008, 2006). For PLS-DA models, cross-validations were performed by testing 100 permutations to test if the models are overfitted. Quality control was performed as previously described (Broadhurst et al., 2018). Data was pareto-scaled and log2-transformed as described in the software. T-tests were performed for calculating statistical significance of lipid concentration changes among the samples taken during the different experiments.

The phylogeny tree was made by extracting the species that are included in this study from Open Tree of Life (Redelings and Holder, 2017) and reconstructed using the Phyton package "scipy" (http://www.scipy.org/) with Ward's cluster analysis. The chemotaxonomic relationships were revealed with aid of the Hierarchical clustering analysis (HCA) function in SIMCA 17. The distance was calculated with Ward method and sorted by index (Ward, 1963).

Barplots were generated using R package "ggplot2" (Wickham, 2009). Heatmap was created by using package "complexheatmap" in R software (version 4.1.0) (Gu et al., 2016), log-transformed relative concentrations of lipid molecular species were used for generating the heatmap, the order of the bryophyte species was manually set to follow the phylogenetic order.

## Credit author statement

YL, experiment design, sample collection, experimental, data analysis, writing manuscript; FFE, supervision of LC/MS analysis. MT, funding acquisition. NC, sample collection and identification. HTS, supervision and funding acquisition. All authors contributed to the manuscript reviewing and editing. All authors approved the final manuscript.

## Declaration of competing interest

The authors declare the following financial interests/personal relationships which may be considered as potential competing interests: Yi Lu reports financial support was provided by Marie Sklodowska-Curie Actions, Innovative Training Networks under European Union Horizon 2020 programme

## Data availability

The data and link is given in the paper.

## Acknowledgements

We acknowledge Dr. Maonian Xu, University of Iceland, for the help of grinding plant materials in liquid nitrogen. Mingzhou Bai, BGI Shenzhen, is acknowledged for preparing phylogeny tree figures. This study is funded by Marie Sklodowska-Curie Actions, Innovative Training Networks under European Union Horizon 2020 programme under grant agreement No. 765115—MossTech.

## Appendix A. Supplementary data

Supplementary data to this article can be found online at https://doi.org/10.1016/j.phytochem.2022.113560.

## References

Al-Hasan, R.H., El-Saadawi, W.E., Ali, A.M., Radwan, S.S., 1989. Arachidonic and eicosapentaenoic acids in lipids of *Bryum bicolor dicks*. Effects of controlled temperature and illumination. Bryologist 92, 178. https://doi.org/10.2307/3243940.

Antonio, C., 2018. Plant Metabolomics, Methods in Molecular Biology. Springer New York, New York, NY. https://doi.org/10.1007/978-1-4939-7819-9.

Arbona, V., Iglesias, D.J., Talón, M., Gómez-Cadenas, A., 2009. Plant phenotype demarcation using nontargeted LC-MS and GC-MS metabolite profiling. J. Agric. Food Chem. 57, 7338–7347. https://doi.org/10.1021/jf9009137.

Asakawa, Y., Ludwiczuk, A., 2018. Chemical constituents of bryophytes: structures and biological activity. J. Nat. Prod. 81, 641–660. https://doi.org/10.1021/acs.jnatprod.6b01046.

Asakawa, Y., Ludwiczuk, A., Nagashima, F., 2013. Chemical constituents of bryophyta. In: Progress in the Chemistry of Organic Natural Products, Progress in the Chemistry of Organic Natural Products. Springer Vienna, Vienna, pp. 563–605. https://doi.org/10.1007/978-3-7091-1084-3_5.

Beike, A.K., Jaeger, C., Zink, F., Decker, E.L., Reski, R., 2014. High contents of very long-chain polyunsaturated fatty acids in different moss species. Plant Cell Rep. 33, 245–254. https://doi.org/10.1007/s00299-013-1525-z.

Broadhurst, D., Goodacre, R., Reinke, S.N., Kuligowski, J., Wilson, I.D., Lewis, M.R., Dunn, W.B., 2018. Guidelines and considerations for the use of system suitability and quality control samples in mass spectrometry assays applied in untargeted clinical metabolomic studies. Metabolomics 14, 72. https://doi.org/10.1007/s11306-018-1367-3.

Bruce, S.J., Jonsson, P., Antti, H., Cloarec, O., Trygg, J., Marklund, S.L., Moritz, T., 2008. Evaluation of a protocol for metabolic profiling studies on human blood plasma by combined ultra-performance liquid chromatography/mass spectrometry: from extraction to data analysis. Anal. Biochem. 372, 237–249. https://doi.org/10.1016/j.ab.2007.09.037.

Cannell, N., Emms, D.M., Hetherington, A.J., MacKay, J., Kelly, S., Dolan, L., Sweetlove, L.J., 2020. Multiple metabolic innovations and losses are associated with major transitions in land plant evolution. Curr. Biol. 30, 1783–1800. https://doi.org/10.1016/j.cub.2020.02.086 e11.

Celis Ramírez, A.M., Amézquita, A., Cardona Jaramillo, J.E.C., Matiz-Cerón, L.F., Andrade-Martínez, J.S., Triana, S., Mantilla, M.J., Restrepo, S., Barrios, A.F.G., Cock, H.de, 2020. Analysis of malassezia lipidome disclosed differences among the species and reveals presence of unusual yeast lipids. Front. Cell. Infect. Microbiol. 10, 1–16. https://doi.org/10.3389/fcimb.2020.00338.

Choudhary, A.K., Sunojkumar, P., Mishra, G., 2017. Fatty acid profiling and multivariate analysis in the genus *Leucas* reveals its nutritional, pharmaceutical and chemotaxonomic significance. Phytochemistry 143, 72–80. https://doi.org/10.1016/j.phytochem.2017.07.007.

Christie, W.W., Han, X., 2012. Gas chromatographic analysis of fatty acid derivatives. Lipid Anal 159–180. https://doi.org/10.1533/9780857097866.159.

Conde, T.A., Couto, D., Melo, T., Costa, M., Silva, J., Domingues, M.R., Domingues, P., 2021. Polar lipidomic profile shows *Chlorococcum amblystomatis* as a promising source of value-added lipids. Sci. Rep. 11, 4355. https://doi.org/10.1038/s41598-021-83455-y.

Dembitsky, V.M., Rezanka, T., 1995. Distribution of diacylglycerylhomoserines, phospholipids and fatty acids in thirteen moss species from Southwestern Siberia. Biochem. Systemat. Ecol. 23, 71–78. https://doi.org/10.1016/0305-1978(95)93660-U.

Dembitsky, V.M., Rezanka, T., 1994. Acetylenic fatty acids of the Dicranaceae. Phytochemistry 36, 685–689. https://doi.org/10.1016/S0031-9422(00)89797-6.

Dührkop, K., Fleischauer, M., Ludwig, M., Aksenov, A.A., Melnik, A.V., Meusel, M., Dorrestein, P.C., Rousu, J., Böcker, S., 2019. Sirius 4: a rapid tool for turning tandem mass spectra into metabolite structure information. Nat. Methods 16, 299–302. https://doi.org/10.1038/s41592-019-0344-8.

Eriksson, L., Kettaneh-Wold, N., Trygg, J., Wikström, C., Wold, S., 2006. Multi- and Megavariate Data Analysis: Part I: Basic Principles and Applications. Umetrics Inc, Department of Chemistry, Faculty of Science and Technology, Umeå University.

Eriksson, L., Trygg, J., Wold, S., 2008. CV-ANOVA for significance testing of PLS and OPLS® models. J. Chemom. 22, 594–600. https://doi.org/10.1002/cem.1187.

Folch, J., Lees, M., Sloane-Stanley, G., 1957. A simple method for the isolation and purification of total lipids from animal tissues. J. Biol. Chem. 226, 497–509.

Gellerman, J.L., Anderson, W.H., Richardson, D.G., Schlenk, H., 1975. Distribution of arachidonic and eicosapentaenoic acids in the lipids of mosses. Biochim. Biophys. Acta Lipids Lipid. Metabol. 388, 277–290. https://doi.org/10.1016/0005-2760(75)90133-2.

Gu, Z., Eils, R., Schlesner, M., 2016. Complex heatmaps reveal patterns and correlations in multidimensional genomic data. Bioinformatics 32, 2847–2849. https://doi.org/10.1093/BIOINFORMATICS/BTW313.

Gupta, A., Barrow, C.J., Puri, M., 2012. Omega-3 biotechnology: thraustochytrids as a novel source of omega-3 oils. Biotechnol. Adv. 30, 1733–1745. https://doi.org/10.1016/j.biotechadv.2012.02.014.

Hansen, C.E., Rossi, P., 1991. Effects of culture conditions on accumulation of arachidonic and eicosapentaenoic acids in cultured cells of *Rhytidiadelphus squarrosus* and *Eurhynchium striatum*. Phytochemistry 30, 1837–1841. https://doi.org/10.1016/0031-9422(91)85024-T.

Hansen Patricia Rossi, C.E., 1990. Arachidonic and eicosapentaenoic acids in Brachytheciaceae and Hypnaceae moss species. Phytochemistry 29, 3749–3754. https://doi.org/10.1016/0031-9422(90)85325-A.

Hartmann, E., Beutelmann, P., Vandekerkhove, O., Euler, R., Kohn, G., 1986. Moss cell cultures as sources of arachidonic and eicosapentaenoic acids. FEBS Lett. 198, 51–55. https://doi.org/10.1016/0014-5793(86)81183-8.

Holčapek, M., Liebisch, G., Ekroos, K., 2018. Lipidomic analysis. Anal. Chem. 90, 4249–4257. https://doi.org/10.1021/acs.analchem.7b05395.

Horai, H., Arita, M., Kanaya, S., Nihei, Y., Ikeda, T., Suwa, K., Ojima, Y., Tanaka, Kenichi, Tanaka, S., Aoshima, K., Oda, Y., Kakazu, Y., Kusano, M., Tohge, T., Matsuda, F., Sawada, Y., Hirai, M.Y., Nakanishi, H., Ikeda, K., Akimoto, N., Maoka, T., Takahashi, H., Ara, T., Sakurai, N., Suzuki, H., Shibata, D., Neumann, S., Iida, T., Tanaka, Ken, Funatsu, K., Matsuura, F., Soga, T., Taguchi, R., Saito, K., Nishioka, T., 2010. MassBank: a public repository for sharing mass spectral data for life sciences. J. Mass Spectrom. 45, 703–714. https://doi.org/10.1002/jms.1777.

Horn, A., Pascal, A., Lončarević, I., Volpatto Marques, R., Lu, Y., Miguel, S., Bourgaud, F., Thorsteinsdóttir, M., Cronberg, N., Becker, J.D., Reski, R., Simonsen, H.T., 2021. Natural products from bryophytes: from basic biology to biotechnological applications. CRC Crit. Rev. Plant Sci. 40, 191–217. https://doi.org/10.1080/07352689.2021.1911034.

Icelandic Institute of Natural History, 2018. Mosses, Hornworts and Liverworts ([WWW Document]).

Icelandic Meteorological Office, 2021. Climatology.

Ingimundardóttir, G.V., Weibull, H., Cronberg, N., Ingimundardottir, G., Weibull, H., Cronberg, N., 2014. Bryophyte colonization history of the virgin volcanic island Surtsey, Iceland. Biogeosciences 11, 4415–4427. https://doi.org/10.5194/bg-11-4415-2014.

Jiao, J., Zhang, Y., 2013. Transgenic biosynthesis of polyunsaturated fatty acids: a sustainable biochemical engineering approach for making essential fatty acids in plants and animals. Chem. Rev. https://doi.org/10.1021/cr300007p.

Kaiser, K.A., Merrywell, C.E., Fang, F., Larive, C.K., 2011. Metabolic Profiling, NMR Spectroscopy in Pharmaceutical Analysis, Methods in Molecular Biology. Humana Press, Totowa, NJ. https://doi.org/10.1007/978-1-61737-985-7.

Kilaru, A., Tamura, P., Isaac, G., Welti, R., Venables, B.J., Seier, E., Chapman, K.D., 2012. Lipidomic analysis of N-acylphosphatidylethanolamine molecular species in Arabidopsis suggests feedback regulation by N-acylethanolamines. Planta 236, 809–824. https://doi.org/10.1007/s00425-012-1669-z.

Kind, T., Liu, K.-H., Lee, D.Y., DeFelice, B., Meissen, J.K., Fiehn, O., 2013. LipidBlast in silico tandem mass spectrometry database for lipid identification. Nat. Methods 10, 755–758. https://doi.org/10.1038/nmeth.2551.

Künzler, K., Eichenberger, W., 1997. Betaine lipids and zwitterionic phospholipids in plants and fungi. Phytochemistry 46, 883–892. https://doi.org/10.1016/S0031-9422(97)81274-5.

Laurin-Lemay, S., Brinkmann, H., Philippe, H., 2012. Origin of land plants revisited in the light of sequence contamination and missing data. Curr. Biol. 22, R593–R594. https://doi.org/10.1016/j.cub.2012.06.013.

Li, Y., Ye, M., Zhang, R., Xu, J., Zhou, C., Yan, X., 2016. Lipid compositions in diatom *Conticribra weissflogii* under static and aerated culture conditions. Phycol. Res. 64, 281–290. https://doi.org/10.1111/pre.12144.

Liu, P., Wang, L., Du, Q., Du, H., 2020. Chemotype classification and biomarker screening of male *Eucommia ulmoides* Oliv. flower core collections using UPLC-QTOF/MS-based non-targeted metabolomics. PeerJ 8, e9786. https://doi.org/10.7717/peerj.9786.

Lu, Y., Eiriksson, F.F., Thorsteinsdóttir, M., Simonsen, H.T., 2021. Effects of extraction parameters on lipid profiling of mosses using UPLC-ESI-QTOF-MS and multivariate data analysis. Metabolomics 17, 96. https://doi.org/10.1007/s11306-021-01847-7.

Lu, Y., Eiriksson, F.F., Thorsteinsdóttir, M., Simonsen, H.T., 2019. Valuable fatty acids in bryophytes—production, biosynthesis, analysis and applications. Plants. https://doi.org/10.3390/plants8110524.

Mikami, K., Hartmann, E., 2004. Lipid metabolism in mosses. In: New Frontiers in Bryology. Springer, Netherlands, pp. 133–155. https://doi.org/10.1007/978-0-306-48568-8_8.

OECD, 2013. OECD compendium of agri-environmental indicators. Int. J. Sustain. High Educ. 14 https://doi.org/10.1108/ijshe.2013.24914daa.011 ijshe.2013.24914daa.011.

Okazaki, Y., Saito, K., 2018. Plant lipidomics using UPLC-QTOF-MS. In: Methods in Molecular Biology. Clifton, N.J., pp. 157–169. https://doi.org/10.1007/978-1-4939-7819-9_11

Parfrey, L.W., Lahr, D.J.G., Knoll, A.H., Katz, L.A., 2011. Estimating the timing of early eukaryotic diversification with multigene molecular clocks. Proc. Natl. Acad. Sci. USA 108, 13624–13629. https://doi.org/10.1073/pnas.1110633108.

Pejin, B., Vujisic, L., Sabovljevic, M., Tesevic, V., Vajs, V., 2011. Fatty acid chemistry of *Atrichum undulatum* and *Hypnum andoi*. Hem. Ind. Ind. 66, 207–209. https://doi.org/10.2298/hemind110918074p.

Pejin, B., Vujisic, Lj, Sabovljevic, A., Sabovljevic, M., Tesevic, V., Vajs, V., 2011. An insight into fatty acid chemistry of Rhytidiadelphus squarrosus (Hedw.). Warnst. Bot. Serbica 35, 99–101.

Peters, K., Balcke, G., Kleinenkuhnen, N., Treutler, H., Neumann, S., 2021. Untargeted in silico compound classification—a novel metabolomics method to assess the chemodiversity in bryophytes. Int. J. Mol. Sci. 22, 3251. https://doi.org/10.3390/ijms22063251.

Peters, K., Treutler, H., Döll, S., Kindt, A.S.D., Hankemeier, T., Neumann, S., Peters, Treutler, Döll, Kindt, Hankemeier, Neumann, 2019. Chemical diversity and classification of secondary metabolites in nine bryophyte species. Metabolites 9, 222. https://doi.org/10.3390/metabo9100222.

Poddar Sarkar, M., Biswas Raha, A., Datta, J., Mitra, S., 2021. Chemotaxonomic and evolutionary perspectives of Bryophyta based on multivariate analysis of fatty acid fingerprints of Eastern Himalayan mosses. Protoplasma 1, 1–13. https://doi.org/10.1007/s00709-021-01723-0.

Redelings, B.D., Holder, M.T., 2017. A supertree pipeline for summarizing phylogenetic and taxonomic information for millions of species, 2017 PeerJ e3058. https://doi.org/10.7717/PEERJ.3058/SUPP-2.

Roy Chowdhuri, S., Biswas Raha, A., Mitra, S., Datta, J., Poddar Sarkar, M., 2018. Dicranin" in the membrane phospholipids of a Dicranaceae and pottiaceae moss member of the eastern himalayan biodiversity hotspot. Lipids 53, 539–545. https://doi.org/10.1002/lipd.12054.

Ruhfel, B.R., Gitzendanner, M.A., Soltis, P.S., Soltis, D.E., Burleigh, J., 2014. From algae to angiosperms–inferring the phylogeny of green plants (Viridiplantae) from 360 plastid genomes. BMC Evol. Biol. 14, 23. https://doi.org/10.1186/1471-2148-14-23.

Smith, C.A., O'maille, G., Want, E.J., Qin, C., Trauger, S.A., Brandon, T.R., Custodio, D. E., Abagyan, R., Siuzdak, G., 2005. METLIN A metabolite mass spectral database. Ther. Drug Monit.

Tosun, A., Nagashima, F., Asakawa, Y., 2015. Terpenoid and steroid components of selected liverworts. Chem. Nat. Compd. 51, 387–391. https://doi.org/10.1007/s10600-015-1294-8.

Tsugawa, H., Arita, M., Kanazawa, M., Ogiwara, A., Bamba, T., Fukusaki, E., 2013. MRMPROBS: a data assessment and metabolite identification tool for large-scale multiple reaction monitoring based widely targeted metabolomics. Anal. Chem. 85, 5191–5199. https://doi.org/10.1021/AC400515S/SUPPL_FILE/AC400515S_SI_003.XLSX.

Tsugawa, H., Nakabayashi, R., Mori, T., Yamada, Y., Takahashi, M., Rai, A., Sugiyama, R., Yamamoto, H., Nakaya, T., Yamazaki, M., Kooke, R., Bac-Molenaar, J. A., Oztolan-Erol, N., Keurentjes, J.J.B., Arita, M., Saito, K., 2019a. A cheminformatics approach to characterize metabolomes in stable-isotope-labeled organisms. Nat. Methods 16, 295–298. https://doi.org/10.1038/s41592-019-0358-2.

Tsugawa, H., Satoh, A., Uchino, H., Cajka, T., Arita, Makoto, Arita, Masanori, 2019b. Mass spectrometry data repository enhances novel metabolite discoveries with advances in computational metabolomics. Metabolites 9, 119. https://doi.org/10.3390/metabo9060119.

Wang, M., Carver, J.J., Phelan, V.V., Sanchez, L.M., Garg, N., Peng, Y., Nguyen, D.D., Watrous, J., Kapono, C.A., Luzzatto-Knaan, T., Porto, C., Bouslimani, A., Melnik, A. V., Meehan, M.J., Liu, W.-T., Crüsemann, M., Boudreau, P.D., Esquenazi, E., Sandoval-Calderón, M., Kersten, R.D., Pace, L.A., Quinn, R.A., Duncan, K.R., Hsu, C.-C., Floros, D.J., Gavilan, R.G., Kleigrewe, K., Northen, T., Dutton, R.J., Parrot, D., Carlson, E.E., Aigle, B., Michelsen, C.F., Jelsbak, L., Sohlenkamp, C., Pevzner, P., Edlund, A., McLean, J., Piel, J., Murphy, B.T., Gerwick, L., Liaw, C.-C., Yang, Y.-L., Humpf, H.-U., Maansson, M., Keyzers, R.A., Sims, A.C., Johnson, A.R., Sidebottom, A.M., Sedio, B.E., Klitgaard, A., Larson, C.B., Boya P, C.A., Torres-Mendoza, D., Gonzalez, D.J., Silva, D.B., Marques, L.M., Demarque, D.P., Pociute, E., O'Neill, E.C., Briand, E., Helfrich, E.J.N., Granatosky, E.A., Glukhov, E., Ryffel, F., Houson, H., Mohimani, H., Kharbush, J.J., Zeng, Y., Vorholt, J.A., Kurita, K.L., Charusanti, P., McPhail, K.L., Nielsen, K.F., Vuong, L., Elfeki, M., Traxler, M.F., Engene, N., Koyama, N., Vining, O.B., Baric, R., Silva, R.R., Mascuch, S.J., Tomasi, S., Jenkins, S., Macherla, V., Hoffman, T., Agarwal, V., Williams, P.G., Dai, J., Neupane, R., Gurr, J., Rodríguez, A.M.C., Lamsa, A., Zhang, C., Dorrestein, K., Duggan, B.M., Almaliti, J., Allard, P.-M., Phapale, P., Nothias, L.-F., Alexandrov, T., Litaudon, M., Wolfender, J.-L., Kyle, J.E., Metz, T.O., Peryea, T., Nguyen, D.-T., VanLeer, D., Shinn, P., Jadhav, A., Müller, R., Waters, K.M., Shi, W., Liu, X., Zhang, L., Knight, R., Jensen, P.R., Palsson, B.Ø., Pogliano, K., Linington, R. G., Gutiérrez, M., Lopes, N.P., Gerwick, W.H., Moore, B.S., Dorrestein, P.C., Bandeira, N., 2016. Sharing and community curation of mass spectrometry data with global natural products social molecular networking. Nat. Biotechnol. 34, 828.

Ward, J.H., 1963. Hierarchical grouping to optimize an objective function. J. Am. Stat. Assoc. 58, 236–244. https://doi.org/10.1080/01621459.1963.10500845.

Wickham, H., 2009. ggplot2, Ggplot2. Springer New York, New York, NY. https://doi.org/10.1007/978-0-387-98141-3.

Wijffels, R.H., Barbosa, M.J., 2010. An outlook on microalgal biofuels (vol 10, pg 67, 2008). Science 330 (80), 913.

Yang, D., Song, D., Kind, T., Ma, Y., Hoefkens, J., Fiehn, O., 2015. Lipidomic analysis of *Chlamydomonas reinhardtii* under nitrogen and sulfur deprivation. PLoS One 10, e0137948. https://doi.org/10.1371/journal.pone.0137948.

Yang, F., Zhao, M., Zhou, L., Zhang, M., Liu, J., Marchioni, E., 2021. Identification and differentiation of wide edible mushrooms based on lipidomics profiling combined with principal component analysis. J. Agric. Food Chem. F. https://doi.org/10.1021/ACS.JAFC.1C02269.

Zhang, P., Wang, X., Wang, T., Zhu, P., LixiaoYang, 2018. The major changes in lipid composition of *Sargassum horneri* during different growth phases. J. Appl. Phycol. 30, 517–523. https://doi.org/10.1007/s10811-017-1219-y.